



Article

Time Series of Remote Sensing Data for Interaction Analysis of the Vegetation Coverage and Dust Activity in the Middle East

Soodabeh Namdari ¹, Ali Ibrahim Zghair Alnasrawi ², Omid Ghorbanzadeh ³, Armin Sorooshian ^{4,5}, Khalil Valizadeh Kamran ^{1,*} and Pedram Ghamisi ³

¹ Department of Remote Sensing and GIS, University of Tabriz, Tabriz 5166616471, Iran; soodabeh_namdari@yahoo.com

² Ministry of Education, General Directorate of Education, Maysan 62003, Iraq; khvaka@yahoo.com

³ Institute of Advanced Research in Artificial Intelligence (IARAI), Landstraßer Hauptstraße 5, 1030 Vienna, Austria; omid.ghorbanzadeh@iarai.ac.at (O.G.); pedram.ghamisi@iarai.ac.at (P.G.)

⁴ Department of Chemical and Environmental Engineering, University of Arizona, P.O. Box 210011, Tucson, AZ 85721, USA; armin@arizona.edu

⁵ Department of Hydrology and Atmospheric Sciences, University of Arizona, P.O. Box 210011, Tucson, AZ 85721, USA

* Correspondence: valizadeh@tabrizu.ac.ir; Tel.: +98-914-412-3849

Abstract: Motivated by the lack of research on land cover and dust activity in the Middle East, this study seeks to increase the understanding of the sensitivity of dust centers to climatic and surface conditions in this specific region. In this regard, we explore vegetation cover and dust emission interactions using 16-day long-term Normalized Difference Vegetation Index (NDVI) data and daily Aerosol Optical Depth (AOD) data from Moderate Resolution Imaging Spectroradiometer (MODIS) and conduct spatiotemporal and statistical analyses. Eight major dust hotspots were identified based on long-term AOD data (2000–2019). Despite the relatively uniform climate conditions prevailing throughout the region during the study period, there is considerable spatial variability in interannual relationships between AOD and NDVI. Three subsets of periods (2000–2006, 2007–2013, 2014–2019) were examined to assess periodic spatiotemporal changes. In the second period (2007–2013), AOD increased significantly (6% to 32%) across the studied hotspots, simultaneously with a decrease in NDVI (−0.9% to −14.3%) except in Yemen–Oman. Interannual changes over 20 years showed a strong relationship between reduced vegetation cover and increased dust intensity. The correlation between NDVI and AOD (−0.63) for the cumulative region confirms the significant effect of vegetation canopy on annual dust fluctuations. According to the results, changes in vegetation cover have an essential role in dust storm fluctuations. Therefore, this factor must be regarded along with wind speed and other climate factors in Middle East dust hotspots related to research and management efforts.

Keywords: time series analysis; remote sensing; dust storm; vegetation monitoring; MODIS Terra



Citation: Namdari, S.; Zghair Alnasrawi, A.I.; Ghorbanzadeh, O.; Sorooshian, A.; Kamran, K.V.; Ghamisi, P. Time Series of Remote Sensing Data for Interaction Analysis of the Vegetation Coverage and Dust Activity in the Middle East. *Remote Sens.* **2022**, *14*, 2963. <https://doi.org/10.3390/rs14132963>

Academic Editor: Ioannis Gitas

Received: 13 May 2022

Accepted: 18 June 2022

Published: 21 June 2022

Publisher's Note: MDPI stays neutral with regard to jurisdictional claims in published maps and institutional affiliations.



Copyright: © 2022 by the authors. Licensee MDPI, Basel, Switzerland. This article is an open access article distributed under the terms and conditions of the Creative Commons Attribution (CC BY) license (<https://creativecommons.org/licenses/by/4.0/>).

1. Introduction

Dust storms are a common phenomenon in the drylands of the Middle East. This atmospheric phenomenon causes adverse environmental and social effects and consequences [1–6]. Dust events in the Middle East arise due to the arid climate and synoptic conditions, and are promoted by increasing desertification, a form of ecological change in response to climate change and human activity [7–9]. Reducing vegetation cover and soil moisture causes desertification that indirectly leads to dust generation [10–15].

Due to the importance of dust storms, there has been extensive research into the relationship between dust intensity and influential factors such as wind speed, temperature, precipitation, vegetation cover, and soil moisture [16–32]. Zou and Zhai [16] analyzed the relationship between vegetation index data and dust storms in China from 1982 to 2001.

They showed that decreasing vegetation index plays an essential role in prevalence of spring dust storms but there is no relationship between vegetation cover and dust storms in some parts of the study area, with little to no vegetation in the desert areas.

Tan [20] analyzed the impacts of vegetative cover on dust-storm levels in China and showed that the association between dust and vegetation became more robust from the dry temperate zone to the sub-humid temperate zone. Parolari et al. [21], using the NDVI anomaly method, analyzed vegetation cover's effect on dust storm generation in the Middle East. Their study's results showed that unusual aridity, combined with unique synoptic weather patterns, are the more probable driver for enhanced dust generation. Li et al. [22] assessed meteorological parameters and NDVI impacts on dust levels in Kuwait from 2001 to 2017. They observed a positive relationship between wind speed and dust levels, and a negative link was observed between dust and vegetation cover.

Kim et al. [23] discovered that the model-derived Saharan dust emissions correlate only with 10 m wind speed over the Sahara and Sahel. In contrast, Sahel dust emissions are associated with 10 m wind speed and vegetation cover. Tai et al. [24] investigated the effect of climatic or land cover changes on interannual changes in dust storms in East Asia from 1982 to 2010. They found that dust emission variability was affected mainly by meteorological parameters, and vegetation density was the second parameter. However, it has a locally important role, especially in the semi-arid and non-desert regions undergoing rapid land cover change and desertification. Yao et al. [25] showed that significant decreases in dust intensity in East Asia correlated with increases in NDVI, soil moisture, precipitation, and reductions in wind speed. In another study, Bao et al. [26] analyzed the spatiotemporal variation of surface and dust emissions using meteorological station data, MODIS NDVI, and soil moisture factors in Xilingol League from 2005 to 2018. The result showed that dust frequency negatively correlates with NDVI and soil moisture. Gholami et al. [27] predicted land susceptibility to dust emissions in Yazd province, central Iran, and they showed that DEM (digital elevation model), vegetation cover, geology, and calcium carbonate are the most critical factors related to dust emissions.

According to our literature review, vegetation cover play important potential roles in dust emissions. The inverse relationship between vegetation cover and dust emission is undeniable, with varying levels of influence in different regions. The deserts of the Middle East region are located across a wide latitude and under different environmental and political conditions, which leads to each parameter having different effect levels in different conditions. Application of multiple spatial-statistical methods and analysis have been made separately for all dust hotspots in the Middle East to understand the importance of vegetation cover in controlling dust emission in hyper-arid, arid, and semi-arid climate conditions.

In this research, we advance the state of knowledge of dust over the Middle East by using up-to-date data, applying different statistical methods to isolate dust hotspots, and subsequently examining the effect of vegetation cover on dust intensity.

2. Materials and Methods

2.1. Study Area

The Middle East has an arid, semi-arid, and in some parts, hyper-arid climate, and can be characterized as dry and hot, with low humidity and rare precipitation during its mild winters and spring [33]. Areas most vulnerable to dust emissions over the Middle East generally include barren/sparsely vegetated areas (semi-arid, arid, and hyper-arid deserts) and dry lake beds with extreme soil moisture deficits (Figure 1) [34,35]. Several desert areas in the Middle East, especially in Saudi Arabia, Iraq, Syria, and Iran, are potential sources of dust [36,37]. Global warming and human activity have caused intensifying dust emissions with different economic and social impacts, such as migration during recent decades [38]. Synoptic analysis shows that dust activity from Baghdad to the Persian Gulf and southwestern Iran stems from the Tigris and Euphrates and their alluvial plain dust sources. This fact demonstrates that the dust crisis in the Middle East strongly depends on

managing water resources in the countries located upstream of the Tigris and Euphrates rivers [39]. In the other regions, it could be said that climate factors have more role in dust variability.

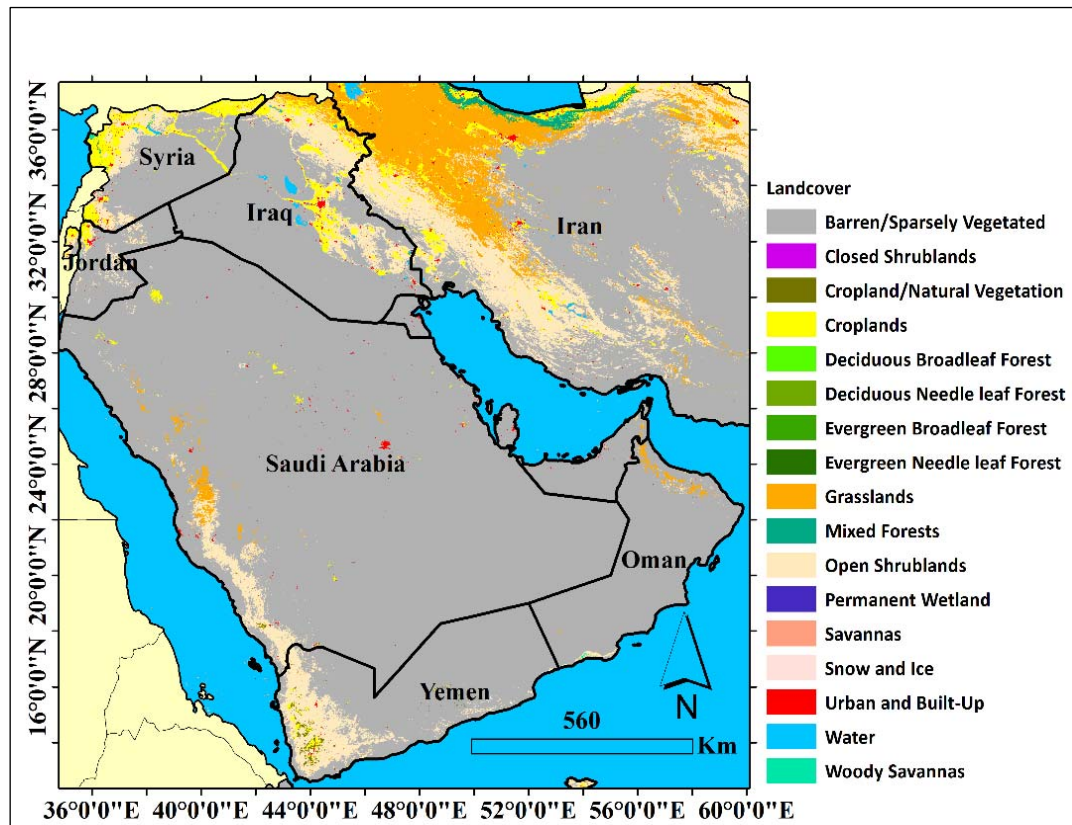


Figure 1. The geographic location of the study area is provided by USGS Land Cover Institute (<https://www.usgs.gov>) (accessed on 10 June 2021).

For further analysis, we divided the study area shown in Figure 1 into several polygons based on different dust hotspots. Large continuous areas with more than 110 dust events per year are mainly considered dust hotspots, but in Saudi Arabia, due to the large area of deserts and also separate areas with more dust generation, 130 events per year are considered.

2.2. Data Selection and Method

This study uses AOD and NDVI data from 2000 to 2019 (accessed on 10 May 2021). Aerosol optical depth (AOD) is a column-integrated measure of radiation extinction by aerosols caused by absorption and scattering. AOD is a critical index in the quantitative calculation of aerosol intensity. Vegetative cover is a factor that has a significant role in soil texture and, consequently, in dust storm emission. The NDVI data are helpful in investigating how vegetative cover affects dust emission in the Middle East. NDVI is one of the most crucial indices for environmental applications relying on the use of the difference of reflectance in near infra red (NIR) and red bands and is defined as [40,41]:

$$NDVI = \frac{B_{NIR} - B_{RED}}{B_{NIR} + B_{RED}}$$

where B (band) represents surface reflectance measurements. We use daily AOD products at 550 nm obtained from Level 2 Collection 6 over land based on the Deep Blue algorithm of MODIS Terra at a resolution of $0.1^\circ \times 0.1^\circ$ (MOD04) [42,43]. NDVI data are based on the MODIS Terra 16-day 500 m NDVI product (MOD13A1) [44,45].

Although we focus on interannual trends from 2000 to 2019, we use daily and 16-day data products for AOD and NDVI, respectively, to obtain data with a higher spatial resolution to subsequently convert to annual time resolution. Mean AOD and NDVI data values have been used to estimate annual data.

There are often pixels with no data, due to issues such as cloud contamination. To compute the mean annual AOD, different interpolation methods have been employed by other studies dealing with no-data pixels [46]. We ignore no-data pixels to eliminate their adverse effects on daily data averaging.

Similar to how daily AOD data were treated and used to scale up to more extended time resolutions, we use 16-day NDVI data to convert to longer time scales, including the yearly resolution, to examine interannual behavior between 2000 and 2019. NDVI maps and time series results will subsequently be compared with AOD to analyze temporal and spatial results, and evaluate vegetation cover effects on dust intensity.

Standard deviation maps were generated based on 20 years of mean-annual AOD data [47–50] to identify areas with the more relative dust activity changes. A similar approach was taken for NDVI data to identify areas with more significant changes in average annual dust intensity that are more vulnerable to vegetation cover changes. To identify dust sources to allow for a more in-depth analysis of those areas, we computed the average number of days per year between 2000 and 2019 with $AOD > 0.6$, considered dusty days. We also examined three time periods between 2000 and 2019 that are relatively evenly spaced (2000–2006, 2007–2013, 2014–2019) to check periodic trends and relationships within the 20-year time frame. Due to climatic and environmental interactions and political decisions, changes can occur in the spatial pattern of dust hotspots in medium-term periods because of the delays in affecting dust emission for some parameters; one-year periods are too short. Therefore, we aim to infer insights into the medium-term impacts of vegetation change on dust intensity variability by analyzing periodical changes.

To further investigate the statistical relationship between vegetation and dust intensity on an annual scale, correlation analysis between these parameters was performed in each dust hotspot and cumulatively for the whole study area

3. Results

Standard deviation maps for AOD show spatial trends in relative dust intensity in the study area (Figure 2a), with higher values in the standard deviation map showing areas more vulnerable to dust storms. Enhanced values were observed for an extensive area extending from the western part of Syria to the southwest of Iran (Khuzestan), and south of Saudi Arabia, northwest Iran, and the center of Iran. The highest standard deviations in the NDVI map (Figure 2b) extend from western Syria to southwestern Iran. A key detail is that these areas of tremendous variability in NDVI do not overlap much with regions in the AOD map with the highest variability. Over large swaths of Saudi Arabia, including the south and eastern areas, close changes in vegetation cover were negligible despite the high annual variability of dust intensity. According to Figure 2a,b, there are different relationships between NDVI and AOD. Consequently, we now compare different sub-regions exhibiting differing relationships between AOD and NDVI.

3.1. Spatio-Temporal Analysis

Boxes labeled A and C in Figure 2a show the relative change in AOD compared to a significant change in NDVI. Boxes B, F, G, and I exhibit high variability in AOD, whereas the NDVI map does not show such a high level of change. Boxes D and E exhibit high relative AOD changes, coinciding with high relative NDVI changes. Box H encompassing Yemen exhibits low changes in AOD and NDVI.

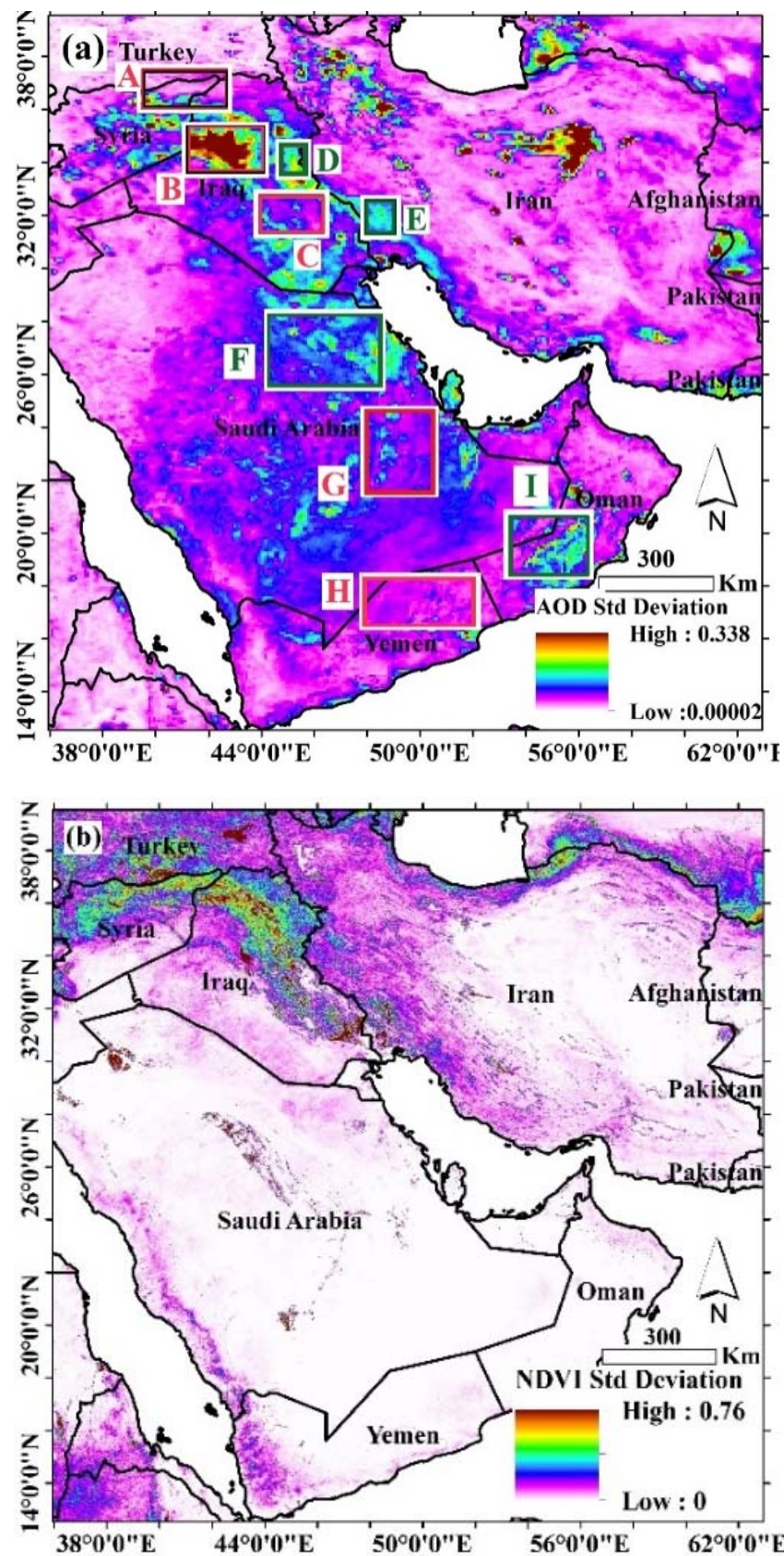


Figure 2. (a) Inter-annual MODIS Terra AOD standard deviation between 2000 and 2019 and (b) inter-annual standard deviation of NDVI extracted based on 16-day MODIS NDVI products. Highlighted boxes in the left panel indicate areas exhibiting varying relationships between AOD and NDVI.

For more investigation, Figure 3 shows dust hotspots which were computed based on daily AOD data from 2000 to 2019. Eight major dust hotspots (yellow to red indicate the most frequent days with AOD > 0.6) in Syria, Iraq, Iran, Saudi Arabia, and Yemen–Oman. These dust hotspots are distributed in different conditions of both climate regime and socio-economic status related to impacts on desertification such as war, dam building, and farming management. The eight hot spots are analyzed separately in this study. As shown in Figure 4, these areas are associated with the barren/sparsely vegetated land-type class.

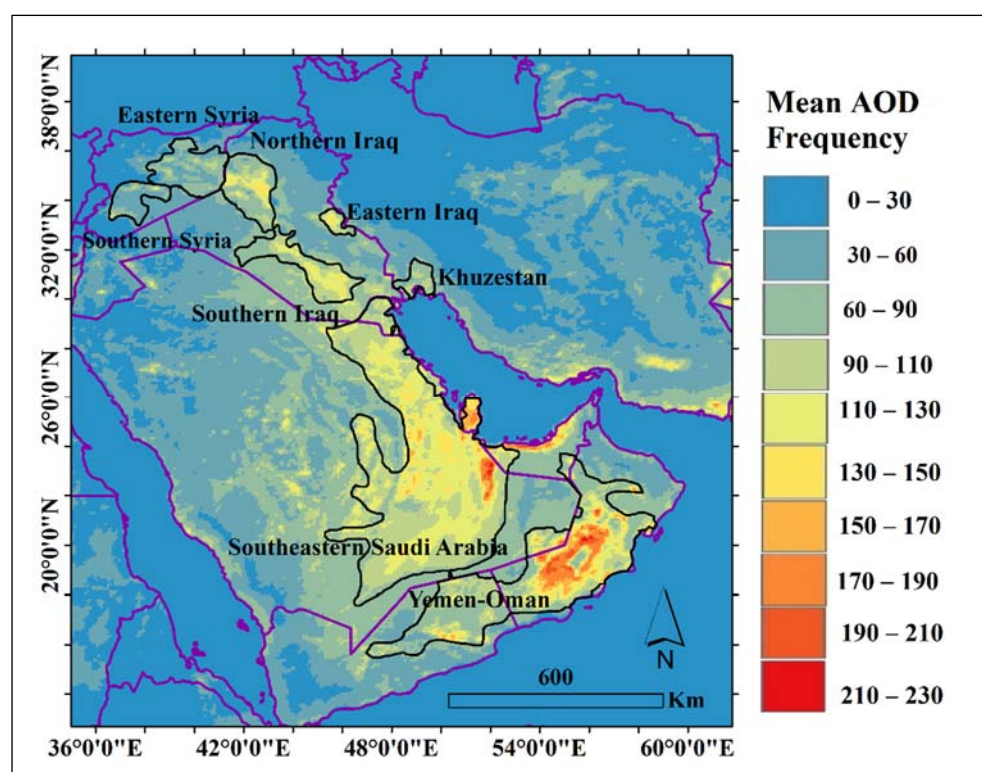


Figure 3. Eight dust hotspots labeled by name were computed based on the mean annual frequency (in days) of MODIS AOD exceeding 0.6 between 2000 and 2019.

To investigate the exact spatial and temporal distribution of dust hotspots and associated NDVI over the 20-year time frame of this study, we take a closer look at AOD and NDVI relationships over three shorter periods: 2000–2006, 2007–2013, 2014–2019. We specifically compare spatiotemporal trends in the relationship between mean values of AOD and NDVI in these three sub-periods (Figure 5 and Tables 1 and 2).

Table 1. Mean AOD for three periods (2000–2006, 2007–2013, 2014–2019) in different dust hotspot regions labeled in Figure 4 and the relative change between the 1st and subsequent periods.

AOD	(2000–2006)	(2007–2013)	(2014–2019)	% Change: 1st (2000–2006) to 2nd Period (2007–2013)	% Change: 1st (2000–2006) to 3rd Period (2014–2019)
East of Syria	0.37	0.44	0.39	19.24%	4.97%
South of Syria	0.38	0.41	0.35	6.86%	−8.47%
North of Iraq	0.42	0.55	0.44	32.52%	4.50%
East of Iraq	0.44	0.53	0.45	21.22%	2.45%
South of Iraq	0.46	0.49	0.46	5.47%	0.11%
Khuzestan	0.41	0.46	0.42	12.02%	2.43%
South East of Saudi Arabia	0.49	0.55	0.50	12.14%	2.29%
Yemen–Oman	0.50	0.53	0.51	6.86%	2.25%

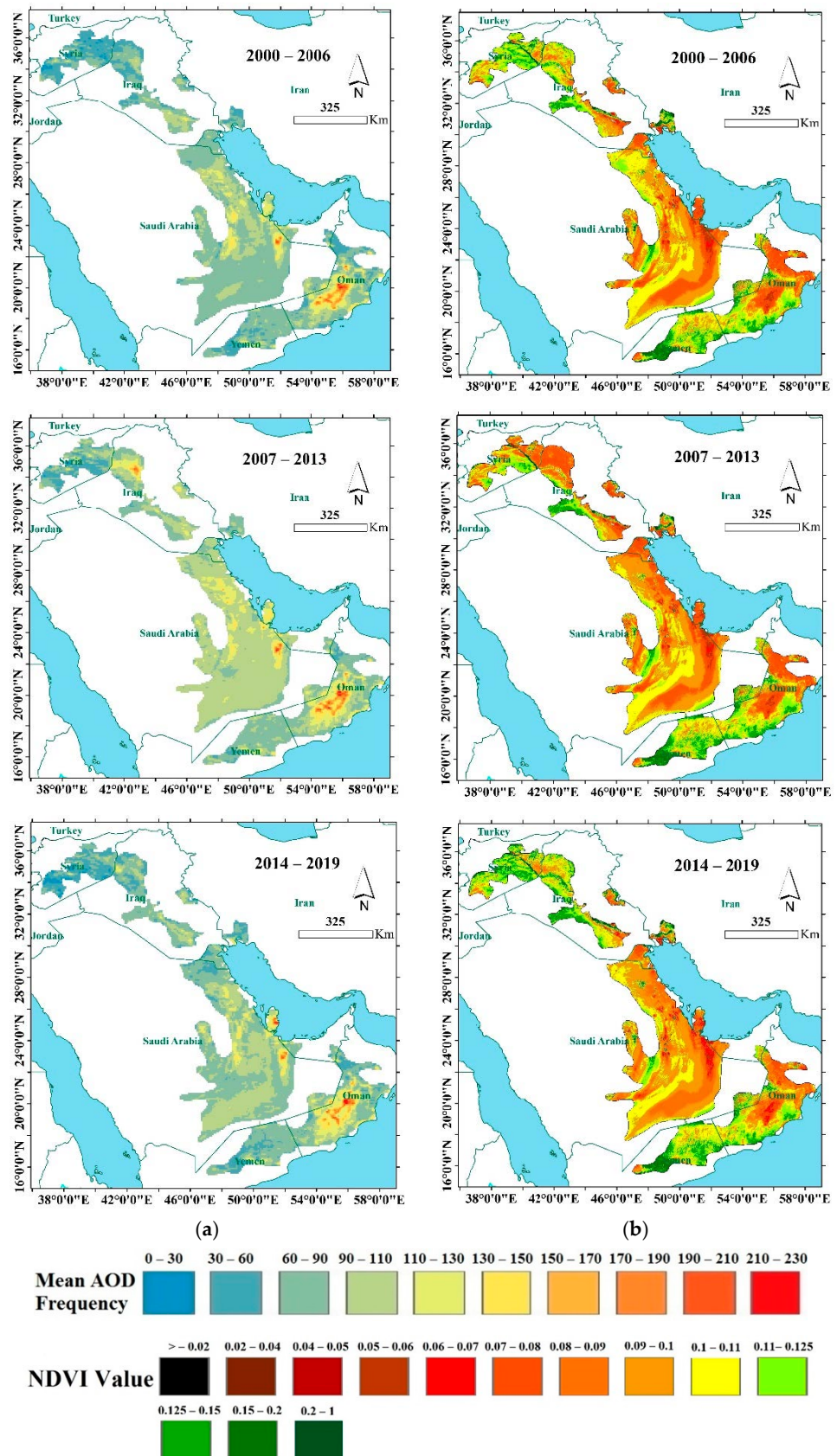


Figure 4. (a) AOD and (b) NDVI for three different periods (2000–2006, 2007–2013, 2014–2019) based on daily MODIS AOD data and 16-day MODIS NDVI data, respectively.

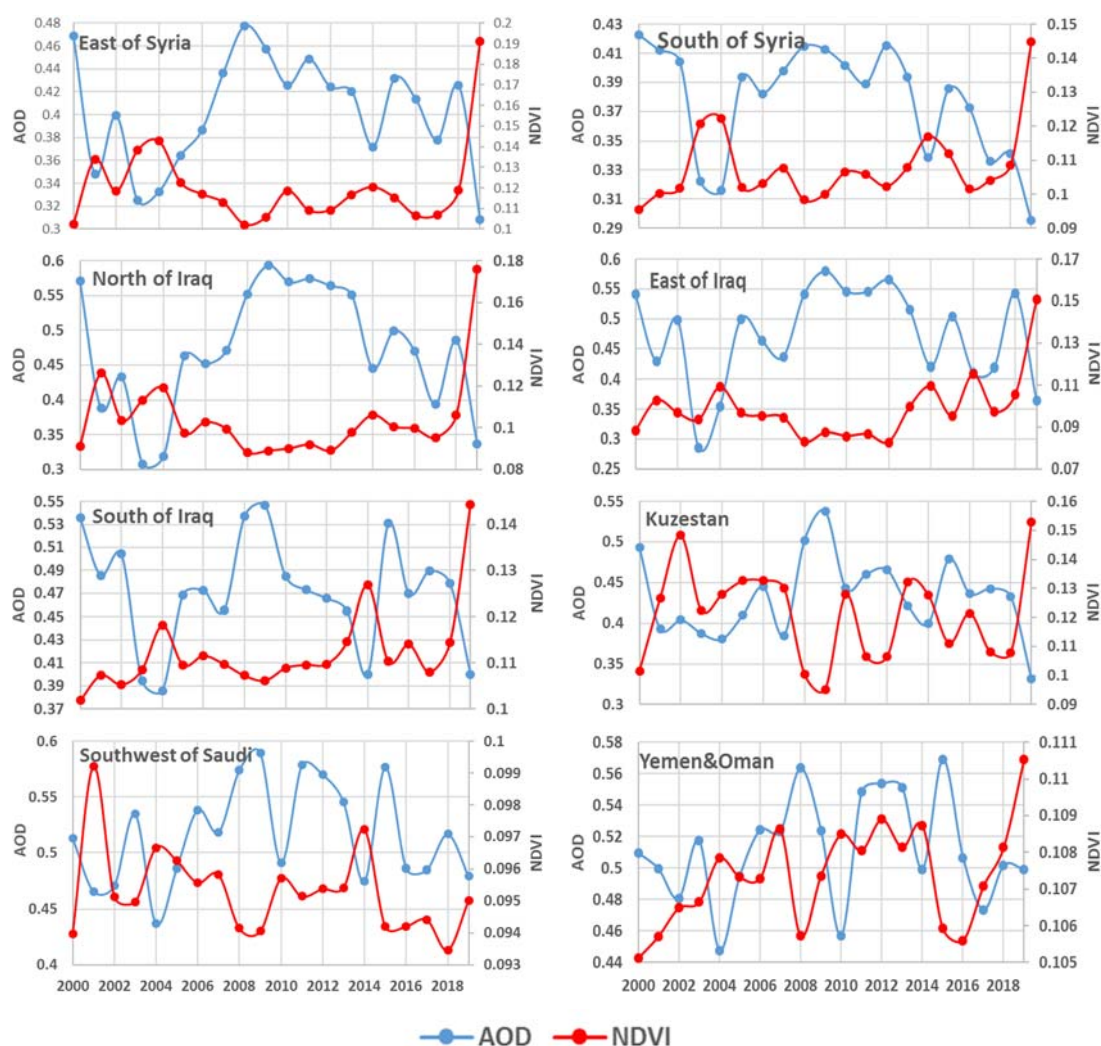


Figure 5. Time series interannual variation in annual mean MODIS Terra AOD and NDVI.

Table 2. Correlation results between AOD and NDVI based on eight hot spots between 2000 and 2019.

	R (p Value)		R (p Value)
East of Syria	−0.80 (0.00)	South of Iraq	−0.65 (0.00)
South of Syria	−0.83 (0.00)	South East of Saudi Arabia	−0.50 (0.00)
North of Iraq	−0.82 (0.00)	Khuzestan	−0.87 (0.00)
East of Iraq	−0.57 (0.00)	Yemen—Oman	−0.13 (0.17)

There are considerable changes in AOD for all eight hotspots from the first to the second period (5.47 to 32.52%), but with dampened changes when comparing the first to the third period (−8.47 to 4.97%). Similarly, more considerable changes occur for NDVI between the first and second period (−14.30 to −2.34%) except in Saudi Arabia and Yemen—Oman (−0.94 to 1.13%), followed by different types of changes between the first and third period with many regions exhibiting a relative increase in NDVI.

Figure 5 shows that the spatial distribution of dust hotspots did not change between the three study periods, coinciding with areas characterized by low vegetation cover. For many hotspots, increases in AOD coincide with a reduction in vegetative cover. This increase is perhaps most evident in northern and southern parts of Iraq, southeastern Saudi Arabia, and Yemen—Oman. In contrast, vegetation remains relatively low in the northeast of Yemen—Oman, but AOD did not reveal very high values.

When comparing the second and first periods, NDVI decreased in the north of the Middle East (e.g., Iraq, Syria, and Iran). There were no significant changes in Saudi Arabia and Yemen–Oman, but there was a slight increase in Yemen–Oman. When comparing the third and first periods, NDVI still showed an overall decrease in the southeast of Saudi Arabia, southern Iraq, and Khuzestan. In other areas, NDVI increased to 15.12% (in eastern Iraq).

Results in Figure 5 and Tables 1 and 2 indicate that in the northern part of Iraq, dust intensity (i.e., AOD) exhibited the most significant relative increase in the second period among all areas (32.52%), and these changes coincided with the most significant decrease in vegetation cover (−14.30%). Comparing the third period to the first one, the NDVI change was 5.85%, simultaneous with an AOD change of 4.50%. Despite an increase in vegetative cover, dust intensity did not decrease. The situation in eastern Syria is almost similar to that in northern Iraq. A 19.24% increase in AOD in the second period was accompanied by a decrease in vegetation cover (−12.04%).

The relationship between vegetation cover and dust intensity is pronounced in south Syria. A 6.86% increase in AOD in the second period was simultaneous with a 2.34% decrease in NDVI. This negative relation was preserved by comparing the third and first periods (−8.47% in AOD and 7.61% in NDVI).

The east of Iraq experienced a considerable increase in AOD in the second period compared to the first period (21.22%), accompanied by a 9.16% reduction in NDVI. Although there is a minor change in the third period in AOD (2.45%), the NDVI change was significant (15.12%), suggesting that the enhancement in AOD was dampened in the third period, potentially owing to a substantial increase in NDVI.

The south of Iraq exhibited the lowest increase in AOD compared to other areas in the second period (5.47%). This value is even lower (0.11%). The relationship between NDVI and AOD is more evident in the second period. NDVI decreased by −8.48%, with less of a relationship in the third period as NDVI decreased by 8.86% compared to the first period.

In Khuzestan, dust intensity increased during the second period (12.02%), and vegetation cover decreased (−10.40%). The negative relationship between the two parameters continued into the third period (2.43% and −4.46% for AOD and NDVI, respectively).

Figure 6 summarizes the interannual variation of dust intensity and vegetation cover based on annual mean values of AOD and NDVI for individual years during the study period. The year 2000 was considered one of the most polluted years in terms of dust intensity, which corresponds to one of the lowest (if not the single lowest) values of NDVI of any year for the various hotspots. Between 2001 and 2004, when dust significantly decreased, vegetation cover in many areas increased compared to 2000. Compared to the first few years, there was an increasing trend in dust intensity from 2005 to 2009. This rising trend continued in Syria and Iraq hotspots until 2013, but Saudi Arabia and Yemen–Oman exhibited a significant reduction in AOD in 2010. Between 2006 and 2019, the inverse relationship between AOD and NDVI is clear for all hotspots. In 2014, the sharp decrease in AOD was accompanied by a high increase in NDVI. In 2018, when there was a significant rise in AOD in all areas (especially in eastern Syria and northern and eastern Iraq), there was a substantial decrease in NDVI. Although in 2019, with the considerable increase in NDVI (compared to other years' values) in Syria, Iraq, and Iran, AOD decreased significantly. However, this decrease is not as pronounced in southeastern Saudi Arabia and Yemen–Oman. This may be due to other parameters' simultaneous influence, such as wind speed.

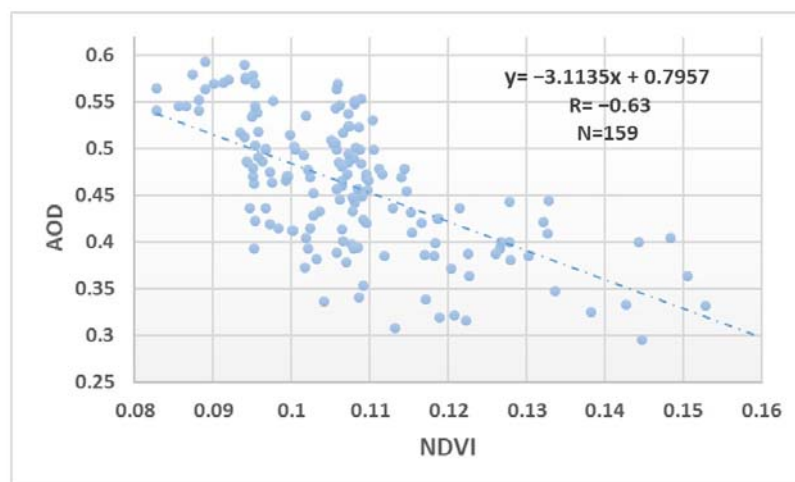


Figure 6. Correlation between AOD and NDVI for all dust hotspots between 2000 and 2019.

3.2. Statistical Analysis

The correlation analysis of vegetation cover and dust intensity for each dust hotspot on an annual scale (Table 2), as well as cumulatively (Figure 6), shows an inverse correlation with statistical significance in each dust hotspot except Yemen–Oman. Aside from Yemen–Oman ($R = -0.13$, p value = 0.17), correlation coefficients range from -0.50 to -0.87 , with the strongest relationship in Khuzestan.

The correlation intensity between NDVI and AOD is -0.63 for the cumulative region (Figure 6), which shows the significant effect of vegetation canopy on annual dust fluctuations. According to Table 2, dust dependence on vegetation cover is less in the dust hotspots that show a lower vegetation index value (such as Yemen–Oman).

4. Discussion

To better understand the causes of dust fluctuations in the Middle East, this study firstly aimed to identify dust hotspots using long-term daily data. According to the results, extracted dust hotspots are consistent with the spatial distribution of dust emission sources extracted by applying SEVIRI geostationary at 15 min temporal resolution and dust storm frequency reported by visibility static data overall in the study areas. This provides confidence in the accuracy of results in the present study [50,51]. Cao et al. [52] applied multiple data types (climate data, trajectory models, and MODIS images) to extract sand and dust storm sources. They extracted six main clusters that were recognized as dust sources, for which the Tigris–Euphrates plain, eastern Syria, and the Iran–Iraq border were identified as severe dust and sand sources, while Saudi Arabia’s fine sands did not qualify as a severe SDS source. The result of the present study on the dust source determination issue agrees with their study for several parts of Iran, Syria, Saudi Arabia, and the southwest of Iran. Ginoux et al. [53] attempted to determine dust hotspots seasonally using mean medium-term data (2003–2009) at a global scale. According to their results, the distribution of dust sources changes in different seasons in the Middle East. These changes are due to atmospheric circulations in different seasons that affect the dust source determination results on a medium-term temporal scale, which would be missed if such data were analyzed in shorter temporal scales.

In the second step, we examined relationships between dust intensity and vegetation cover over 20 years from 2000 to 2019. According to the spatial distribution of standard deviation maps, the vulnerability of dust emission to vegetation cover changes is not the same in different regions. Selected sub-regions showed various links between AOD and NDVI variability. The relationship between dust intensity and vegetation cover is apparent for some dust hotspots such as Khuzestan and eastern Iraq. In contrast, Yemen and Saudi Arabia did not show any association largely because these are hyper-arid desert regions

with very little vegetation. A closer look was taken at the long-term trends in AOD and NDVI for eight major dust hotspots as identified based on high annual frequencies of days with AOD exceeding 0.6. The same behavior in AOD and NDVI fluctuations could show the same climate and surface situation domain. The temporal analysis of AOD and NDVI over 20 years shows no increasing or decreasing trend in dust intensity and vegetation cover in the Middle East. Year-to-year slope changes in AOD and dust fluctuations during the 20 years in Syria, Iraq, and Khuzestan have been very similar. This similarity can be seen between southeastern Saudi Arabia and Yemen–Oman. This similarity in behavior of NDVI fluctuations is between Syria and Iraq hotspots. For all dust sources, there was a negative relationship between vegetation cover and dust intensity over the 20 years examined [25–27]. Statistical analysis of the correlation between vegetation cover and dust intensity confirms the results of the spatio-temporal study. It indicates a strong correlation between dust emission and vegetation cover, especially in areas with more vegetation. The results of Zou and Zhai [16,20] and Tan's studies also show that the relationship between vegetation cover and dust intensity becomes more robust, increasing humidity and consequently, increasing vegetation cover.

A comparison of our results with previous work done by Namdari et al. [54] shows that in contrast to temperature and precipitation parameters, vegetation cover is an indicator with a stronger relationship with dust for this study region. This relation owes to the effects of parameters such as precipitation and temperature on dust emission that are more indirect. That vegetation cover effect arises from those other parameters and is more closely linked to dust intensity. This has implications for forecasting dust activity over long-term periods as vegetation cover can be a reasonable proxy for dust erosion vulnerability in this and other study regions. It could be possible for all researchers to achieve a database used in this study for a long time and evaluate the vegetation cover impact on dust intensity in the other desert areas. Investigating vegetation cover and dust emission in different parts of the world could help reveal the consistency in such a relationship with implications for conservation and restoration of vegetation cover in each dust hotspot. Future research is warranted to put conclusions of this work on firmer ground.

5. Conclusions

The present study on interaction analysis of the vegetation coverage and dust activity in the Middle East yielded the following conclusions:

- Eight dust hotspots were extracted in Syria, Iraq, Iran, Saudi Arabia, and Yemen using long-term daily AOD products in the Middle East.
- According to standard deviation maps, AOD changes in coincidence with NDVI changes.
- The dust hotspots' spatial distribution did not change during the three study periods.
- During three study periods, increases in AOD coincide with a reduction in vegetative cover.
- Interannual variation in annual mean AOD and NDVI support a significant negative effect of vegetation cover on dust activity in twenty consecutive years in all dust hotspots.
- The statistical relationship between vegetation and dust intensity shows a significant relationship based on the correlation coefficient between NDVI and AOD.

According to the results of this study, the most vulnerable areas to changes in vegetation cover are East of Syria, South of Syria, North of Iraq, South of Iraq, and Khuzestan. Thus, it is crucial to pay attention to preserving and restoring vegetation in these areas to reduce the consequences of dust storms.

Author Contributions: Conceptualization, S.N., A.I.Z.A. and O.G.; Data curation, S.N.; Investigation, S.N., A.I.Z.A. and K.V.K.; Methodology, S.N., A.I.Z.A. and K.V.K.; Supervision, K.V.K., P.G. and A.S.; Validation, S.N. and K.V.K.; Visualization, S.N. and O.G.; Writing—original draft, S.N., A.I.Z.A. and K.V.K.; Writing—review and editing, P.G. and A.S. All authors have read and agreed to the published version of the manuscript.

Funding: This research was funded by the Institute of Advanced Research in Artificial Intelligence (IARAI) GmbH. The works of S.N. and K.V.K. were supported by the research grant of the University of Tabriz, grant number 4647.

Data Availability Statement: The data used in this research were obtained from the following websites: MOD04: <http://ladsweb.nascom.nasa.gov/data> (accessed on 10 May 2021) and MOD13A1: <http://ladsweb.nascom.nasa.gov/data> (accessed on 15 May 2021).

Acknowledgments: The authors are grateful to the anonymous referees for their helpful comments/suggestions that have helped us improve an earlier version of the manuscript. The authors also appreciate the Atmospheric Data Center and the Goddard Center for providing the MODIS satellite data and analysis infrastructure as a part of NASA’s Goddard Earth Sciences (GES).

Conflicts of Interest: The authors declare no conflict of interest.

References

- Bollen, J.; Hers, S.; van der Zwaan, B. An integrated assessment of climate change, air pollution, and energy security policy. *Energy Policy* **2010**, *38*, 4021–4030. [[CrossRef](#)]
- Srikanth, M.; Satyanarayana, A.N.V.; Venkata Srinivas, C. Simulation of atmospheric dispersion of NOX over complex terrain region of Ranchi with FLEXPART-WRF by incorporation of improved turbulence intensity relationships. *Atmos. Environ.* **2015**, *123*, 139–155.
- Morelli, X.; Rieux, C.; Cyrus, J.; Forsberg, B.; Slama, R. Air pollution, health and social deprivation: A fine-scale risk assessment. *Environ. Res.* **2016**, *147*, 59–70. [[CrossRef](#)]
- Middleton, N.; Kang, U. Sand and Dust Storms: Impact Mitigation. *Sustainability* **2017**, *9*, 1053. [[CrossRef](#)]
- Guan, Q.; Li, F.; Yang, L.; Zhao, R.; Yang, Y.; Luo, H. Spatial-temporal variations and mineral dust fractions in particulate matter mass concentrations in an urban area of northwestern China. *J. Environ. Manag.* **2018**, *222*, 95–103. [[CrossRef](#)]
- Soleimani, Z.; Teymouri, P.; Darvishi Bolorani, A.; Mesdaghinia, A.; Middleton, N.; Griffin, D.W. An overview of bioaerosol load and health impacts associated with dust storms: A focus on the Middle East. *Atmos. Environ.* **2020**, *223*, 117–187. [[CrossRef](#)]
- Schilling, J.; Hertig, E.; Trambly, Y.; Scheffran, J. Climate change vulnerability, water resources and social implications in North Africa. *Reg. Environ. Chang.* **2020**, *20*, 15. [[CrossRef](#)]
- Middleton, N.; Kashani, S.S.; Attarchi, S.; Rahnama, M.; Mosalman, S.T. Synoptic Causes and Socio-Economic Consequences of a Severe Dust Storm in the Middle East. *Atmosphere* **2021**, *12*, 1435. [[CrossRef](#)]
- Al-Dousari, A.; Domenico, D.; Modi, A. Types, indications and impact evaluation of sand and dust storms trajectories in the Arabian Gulf. *Sustainability* **2017**, *9*, 1526. [[CrossRef](#)]
- Engelstaedter, S.; Kohfeld, K.E.; Tegen, I.; Harrison, S.P. Controls of dust emissions by vegetation and topographic depressions: An evaluation using dust storm frequency data, *Geophys. Res. Lett.* **2003**, *30*, 1294. [[CrossRef](#)]
- Miri, A.; Moghaddamnia, A.; Pahlavanravi, A.; Panjehkeh, N. Dust storm frequency after the 1999 drought in the Sistan region, Iran. *Clim. Res.* **2010**, *41*, 83–90. Available online: <http://www.jstor.org/stable/24870477> (accessed on 1 April 2021). [[CrossRef](#)]
- Fan, B.; Guo, L.; Li, N.; Chen, J.; Lin, H.; Zhang, X.; Shen, M.; Rao, Y.; Wang, C.; Ma, L. Earlier vegetation green-up has reduced spring dust storms. *Sci. Rep.* **2014**, *4*, 6749. [[CrossRef](#)] [[PubMed](#)]
- Yu, Y.; Notaro, M.; Wang, F.; Mao, J.; Shi, X.; Wei, Y. Observed positive vegetation-rainfall feedbacks in the Sahel dominated by a moisture recycling mechanism. *Nat. Commun.* **2017**, *8*, 1873. [[CrossRef](#)] [[PubMed](#)]
- Vali, A.A.; Mousavi, S.H.; Zamani, E. Statistical analysis of occurrence frequency of dust storms in Yazd province and its modeling based on climatic elements and vegetation cover. *J. Spat. Anal. Environ. Hazards* **2019**, *6*, 121–142. Available online: <http://jsaeh.khu.ac.ir/article-1-2792-en.html> (accessed on 5 April 2021). [[CrossRef](#)]
- Jiang, L.; Jiapaer, G.; Bao, A.; Kurban, A.; Guo, H.; Zheng, G.; De Maeyer, P. Monitoring the long-term desertification process and assessing the relative roles of its drivers in Central Asia. *Ecol. Indic.* **2019**, *104*, 195–208. [[CrossRef](#)]
- Zou, X.K.; Zhai, P.M. Relationship between vegetation coverage and spring dust storms over northern China. *J. Geophys. Res.* **2004**, *109*, D03104. [[CrossRef](#)]
- Gong, S.L.; Zhang, X.Y.; Zhao, T.L.; Barrie, L.A. Sensitivity of Asian dust storm to natural and anthropogenic factors. *Geophys. Res. Lett.* **2004**, *31*, L07210. [[CrossRef](#)]
- Yang, B.; Bräuning, A.; Zhang, Z.; Dong, Z.; Esper, J. Dust storm frequency and its relation to climate changes in Northern China during the past 1000 years. *Atmos. Environ.* **2007**, *41*, 9288–9299. [[CrossRef](#)]

19. Yu, H.; Chin, M.; Yuan, T.; Bian, H.; Remer, L.A.; Prospero, J.M.; Omar, A.; Winker, D.; Yang, Y.; Zhang, Y.; et al. The fertilizing role of African dust in the Amazon rainforest: A first multiyear assessment based on CALIPSO LIDAR observations. *Geophys. Res. Lett.* **2015**, *42*, 1984–1991. [[CrossRef](#)]
20. Tan, M. Exploring the relationship between vegetation and dust-storm intensity (DSI) in China. *J. Geogr. Sci.* **2016**, *26*, 387–396. [[CrossRef](#)]
21. Parolari, A.J.; Li, D.; Bou-Zeid, E.; Katul, G.G.; Assouline, S. Climate, not conflict, explains extreme Middle East dust storm. *Environ. Res. Lett.* **2016**, *11*, 114013. [[CrossRef](#)]
22. Li, J.; Garshick, E.; Al-Hemoud, A.; Huang, S.; Koutrakis, P. Impacts of meteorology and vegetation on surface dust concentrations in Middle Eastern countries. *Sci. Total Environ.* **2020**, *712*, 136597. [[CrossRef](#)] [[PubMed](#)]
23. Kim, D.; Chin, M.; Remer, L.A.; Diehl, T.; Bian, H.; Yu, H.; Brown, M.E.; Stockwell, W.R. Role of surface wind and vegetation cover in multi-decadal variations of dust emission in the Sahara and Sahel. *Atmos. Environ.* **2017**, *148*, 282–296. [[CrossRef](#)]
24. Tai, A.P.K.; Ma, P.H.L.; Chan, Y.C.; Chow, M.K.; Ridley, D.A.; Kok, J.F. Impacts of climate and land cover variability and trends on springtime East Asian dust emission over 1982–2010: A modeling study. *Atmos. Environ.* **2021**, *254*, 118348. [[CrossRef](#)]
25. Yao, W.; Gui, K.; Wang, Y.; Che, H.; Zhang, X. Identifying the dominant local factors of 2000–2019 changes in dust loading over East Asia. *Sci. Total Environ.* **2021**, *777*, 146064. [[CrossRef](#)]
26. Bao, C.; Yong, M.; Bi, L.; Gao, H.; Li, J.; Bao, Y. Impacts of underlying surface on the dusty weather in central Inner Mongolian steppe, China. *Earth Space Sci.* **2021**, *8*, e2021EA001672. [[CrossRef](#)]
27. Gholami, H.; Mohamadifar, A.; Rahimi, S.; Kaskaoutis, D.G.; Collins, A.L. Predicting land susceptibility to atmospheric dust emissions in central Iran by combining integrated data mining and a regional climate model. *Atmos. Pollut. Res.* **2021**, *12*, 172–187. [[CrossRef](#)]
28. Rezazadeh, M.; Irannejad, P.; Shao, Y. Climatology of the Middle East dust events. *Aeolian Res.* **2013**, *10*, 103–109. [[CrossRef](#)]
29. Gherboudj, I.; Beegum, S.N.N.; Ghedira, H. Identifying natural dust source regions over the Middle-East and North-Africa: Estimation of dust emission potential. *Earth Sci. Rev.* **2017**, *165*, 342–355. [[CrossRef](#)]
30. Anoruo, C.M. Sub-seasonal aerosol characterization at the Middle East regions of AERONET site. *Urban Clim.* **2021**, *37*, 100827. [[CrossRef](#)]
31. Darvishi Bolorani, A.; Papi, R.; Soleimani, M.; Karami, L.; Amiri, F.; Neysani Samany, N. Water bodies changes in Tigris and Euphrates basin has impacted dust storms phenomena. *Aeolian Res.* **2021**, *50*, 100698. [[CrossRef](#)]
32. Al Ameri, I.D.S.; Briant, R.; Engels, S. Drought severity and increased dust storm frequency in the Middle East: A case study from the Tigris-Euphrates alluvial plain, central Iraq. *Weather* **2019**, *74*, 416–426. [[CrossRef](#)]
33. Lelieveld, J.; Beirle, S.; Hörmann, C.; Stenchikov, G.; Wagner, T. Abrupt recent trend changes in atmospheric nitrogen dioxide over the Middle East. *Sci. Adv.* **2015**, *1*, 1500498. [[CrossRef](#)] [[PubMed](#)]
34. Alizadeh-Choobari, O. Impact of aerosol number concentration on precipitation under different precipitation. *Meteorol. Appl.* **2018**, *25*, 596–605. [[CrossRef](#)]
35. Javadian, M.; Behrangi, A.; Sorooshian, A. Impact of drought on dust storms: Case study over Southwest Iran. *Environ. Res. Lett.* **2019**, *14*, 124029. [[CrossRef](#)]
36. Goudie, A.S.; Middleton, N.J. *Desert Dust in the Global System*; Springer Science & Business Media: Berlin/Heidelberg, Germany, 2006.
37. Rashki, A.; Kaskaoutis, D.G.; Sepehr, A. Statistical evaluation of the dust events at selected stations in southwest Asia: From the Caspian Sea to the Arabian Sea. *Catena* **2018**, *165*, 590–603. [[CrossRef](#)]
38. Hafeznia, M.R.; Taheri, A.; FarajzadehAsl, M. Political Effects Resulting from Dust Storms in Tigris and Euphrates Basins. *Geopolit. Q.* **2017**, *12*, 13–38.
39. Hamidi, M. The key role of water resources management in the middle east dust events. *Catena* **2020**, *187*, 104337. [[CrossRef](#)]
40. Qi, Y.; Ge, J.; Huang, J. Spatial and temporal distribution of MODIS and MISR aerosol optical depth over northern China and comparison with AERONET. *Chin. Sci. Bull.* **2013**, *58*, 2497–2506. [[CrossRef](#)]
41. Xue, J.; Su, B. Significant Remote Sensing Vegetation Indices: A Review of Developments and Applications. *J. Sens.* **2017**, *2017*, 1353691. [[CrossRef](#)]
42. Namdari, S.; Valizadeh Kamran, K.; Sorooshian, A. Analysis of some factors related to dust storms occurrence in the Sistan region. *Environ. Sci. Pollut. Res.* **2021**, *28*, 45450–45458. [[CrossRef](#)]
43. Holben, B.N.; Eck, T.F.; Slutsker, I.; Tanré, D.; Buis, J.P.; Setzer, A.; Vermote, E.; Reagan, J.A.; Kaufman, Y.J.; Nakajima, T.; et al. AERONET—A federated instrument network and data archive for aerosol characterization. *Remote Sens. Environ.* **1998**, *66*, 1–16. [[CrossRef](#)]
44. Levy, R.C.; Remer, L.A.; Kaufman, Y.J. Effects of neglecting polarization on the MODIS aerosol retrieval over land. *IEEE Trans. Geosci. Remote Sens.* **2004**, *42*, 2576–2583. [[CrossRef](#)]
45. Zhang, Y.; Song, C.; Band, L.; Sun, G.; Li, J. Reanalysis of global terrestrial vegetation trends from MODIS products: Browning or greening? *Remote Sens. Environ.* **2017**, *191*, 145–155. [[CrossRef](#)]
46. Ginoux, P.; Garbuzov, D.; Hsu, N.C. Identification of anthropogenic and natural dust sources using Moderate Resolution Imaging Spectroradiometer (MODIS) Deep Blue level 2 data. *J. Geophys. Res.* **2010**, *115*, D05204. [[CrossRef](#)]
47. Fatichi, S.; Ivanov, V.Y.; Caporali, E. Investigating interannual variability of precipitation at the global scale: Is there a connection with seasonality? *J. Clim.* **2012**, *25*, 5512–5523. [[CrossRef](#)]

48. Li, Y.; Wang, F. Thermocline spiciness variations in the tropical Indian Ocean observed during 2003–2014. *Deep Sea Res. Part I Oceanogr. Res. Pap.* **2015**, *97*, 52–66. [[CrossRef](#)]
49. Lennartz, S.T.; Gauss, M.; von Hobe, M.; Marandino, C.A. Monthly resolved modelled oceanic emissions of carbonyl sulfide and carbon disulfide for the period 2000–2019. *Earth Syst. Sci.* **2020**, 389. [[CrossRef](#)]
50. Hennen, M.; White, K.; Shahgedanova, M. An assessment of SEVIRI imagery at various temporal resolutions and the effect on accurate dust emission mapping. *Remote Sens.* **2019**, *11*, 918. [[CrossRef](#)]
51. Middleton, N.J. Dust storms in the Middle East. *J. Arid. Environ.* **1986**, *10*, 83–96. [[CrossRef](#)]
52. Cao, H.; Amiraslani, F.; Liu, J.; Zhou, N. Identification of dust storm source areas in West Asia using multiple environmental datasets. *Sci. Total Environ.* **2015**, *502*, 224–235. [[CrossRef](#)]
53. Ginoux, P.; Prospero, J.M.; Gill, T.E.; Hsu, N.C.; Zhao, M. Global-scale attribution of anthropogenic and natural dust sources and their emission rates based on MODIS Deep Blue aerosol products. *Rev. Geophys.* **2012**, *50*. [[CrossRef](#)]
54. Namdari, S.; Karimi, N.; Sorooshian, A.; Mohammadi, G.; Sehatkashani, S. Impacts of climate and synoptic fluctuations on dust storm activity over the Middle East. *Atmos. Environ.* **2018**, *173*, 265–276. [[CrossRef](#)]